

## AUTOMATED ORIENTATION WITH THREE-DIMENSIONAL MOSAICING

Kazuo Oda

Asia Air Survey Co., Ltd.  
8-10 Tamura-cho, Atsugi-shi, Kanagawa-ken, 243-0016, JAPAN  
EMail: kz.oda@ari.ajiko.co.jp

Commission V, Working Group V/I

**KEY WORDS:** Image Registration, Mosaic, Orientation, Non-linear Optimization.**ABSTRACT**

This paper discusses the feasibility of applying three-dimensional mosaicing method for automated orientation problem. The three-dimensional mosaicing, which is an extension of two-dimensional image mosaicing technique, is regarded as an image registration method for scenes with disparity due to difference of depth. The three-dimensional mosaicing gives orientation parameters in a more general way. Depth parameters at specified mesh points are estimated as well as parameters for geometry of cameras at the same time. We developed a prototype system which executed the three-dimensional mosaicing algorithm with pair of stereo images. Experimental results show that RMS errors of vertical parallax were about 0.5 pixel.

**1. INTRODUCTION**

Existing automated (relative) orientation techniques generally extract feature points in stereo pair images and find correspondence between them without human aid. The quality of orientation, however, mainly depends on how many or how clear the feature points are in the images and how correctly they are extracted and measured.

Three-dimensional mosaicing (3-D mosaicing), which is an extension of two-dimensional image mosaicing technique, is regarded as an image registration method for scenes between which disparity exists due to difference of depth. The 3-D mosaicing can calculate orientation parameters in a more general way. Depth parameters at specified mesh points are estimated as well as parameters for geometry of cameras at the same time.

Although these parameters are described in coordinate system of projective geometry, a normal set of orientation parameters in Euclidean coordinate system can be derived theoretically if internal orientation parameters of stereo pair are given. The 3-D mosaicing does not require extraction of feature points in images; it directly optimizes orientation parameters and depth parameters so that the sum of differences of brightness between corresponding pixels are minimized.

In this paper, after describing image registration technique of 3-D mosaicing, a set of results of the test registration will be shown and feasibility of applying 3-D mosaicing for automated orientation problem will be discussed.

**2. IMAGE REGISTRATION TECHNIQUE OF 3-D MOSAICING****2.1 Image Registration Technique of 2-D Mosaicing**

Two-Dimensional image mosaicing (2-D mosaicing) is an image registration method which can automatically match one image with another. This algorithm assumes that correspondences of cocoanuts between two images  $I$  and  $I'$  is represented by projective transformation:

$$\begin{aligned} x'(x, y, H) &= \frac{h_1x + h_2y + h_3}{h_7x + h_8y + 1} \\ y'(x, y, H) &= \frac{h_4x + h_5y + h_6}{h_7x + h_8y + 1} \end{aligned} \quad (1)$$

where  $(x, y)$  and  $(x', y')$  are coordinates of Image  $I$  and  $I'$ , and  $H(h_1, \dots, h_8)$  is a set of coefficients of projective transformation. In many studies two-dimensional image mosaicing adopts Levenberg-Marquardt (LM) method to calculate  $H(h_1, \dots, h_8)$  automatically. The LM method is a non-linear optimization which is an extension of least square minimization. The LM method can be used to optimize  $H(h_1, \dots, h_8)$  so as to minimize the following evaluation function  $\chi^2(H)$ :

$$\begin{aligned} \chi^2(H) &= \sum_{i=1}^N e_i^2 \\ e_i &= I(x_i, y_i) - I'(x'(x_i, y_i, H), y'(x_i, y_i, H)) \end{aligned} \quad (2)$$

where  $l(x, y)$  and  $l'(x', y')$  are pixel value of image  $l$  and  $l'$ .

Many studies of 2-D image mosaicing employs coarse-to-fine strategy which refines precision by processing series of images structured hierarchically in different scales from coarse to fine. This strategy contributes to avoiding to converge local minimum of  $\chi^2(H)$ , as well as reduces processing time.

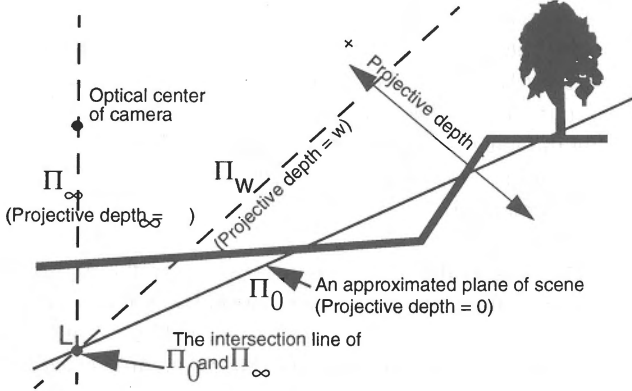


Figure 1: A simple schema of projective depth

## 2.2 3-D Image Mosaicing

The 3-D mosaicing is an extension of 2-D image mosaicing. In 3-D mosaicing, Equation (1) is modified as the following form (Szeliski, 1994):

$$\begin{aligned} x'(x, y, H) &= \frac{h_1 x + h_2 y + h_3 + t_1 \cdot w(x, y)}{h_7 x + h_8 y + 1 + t_3 \cdot w(x, y)} \\ y'(x, y, H) &= \frac{h_4 x + h_5 y + h_6 + t_2 \cdot w(x, y)}{h_7 x + h_8 y + 1 + t_3 \cdot w(x, y)} \end{aligned} \quad (3)$$

where  $(t_1, t_2, t_3)$  is the homogeneous coordinates of the epipole in image  $l'$  where the optical center for image  $l$  is projected, and  $w$  is depth parameter. The 2-D coordinates of the epipole is given by  $(t_1/t_3, t_2/t_3)$ . The parameters  $H$  and  $(t_1, t_2, t_3)$  are called camera parameters because they represent 3-D geometry of cameras.

The depth parameter  $w$  is a special case of generalized disparity (Oda, Kano and Kanade, 1997). If the depth parameter  $w$  is constant, Equation (3) shows simple projective transformation. This means that  $w$  is constant on some plane in 3-D space, and that the parameters  $H(h_1, \dots, h_8)$  are projective transformation in case that  $w = 0$ .

Figure 1 illustrates the concept of depth parameter. The plane  $\Pi_0$  where  $w$  has value 0 and all points are projected by  $H$  between  $l$  and  $l'$ , can be defined arbitrarily in the 3-D space, but it is reasonable to determine  $\Pi_0$  as an plane which approximates the scene of  $l$  and  $l'$ , because the parameters  $H(h_1, \dots, h_8)$  are calculated first in 3-D

mosaicing process so as to roughly register the whole scene.

The depth parameter  $w$  is infinite on the plane  $\Pi_\infty$  which goes through the optical center of image  $l$ . If  $w$  is constant, objects are on a plane which shares a common line  $L$  with  $\Pi_0$  and  $\Pi_\infty$ .

The parameters  $w(x, y)$  and  $(t_1, t_2, t_3)$  can also be calculated by using the LM method. In general,  $w(x, y)$  are estimated with  $n$  control vertices  $P_i(x_i, y_i)$  ( $i=1, 2, \dots, n$ ) in order to reduce the total number of parameters for optimization and the full depth parameters are interpolated from  $w(x_i, y_i)$  by proper method such as spline function (Szeliski, 1994). We have employed planar interpolation, which constructs the scene with planar triangles whose corners are on the control vertices. If  $(x, y)$  is spacially included in a triangle whose corners are control vertices  $(x_i, y_i)$ ,  $(x_j, y_j)$  and  $(x_k, y_k)$ ,  $w(x, y)$  is denoted as following:

$$w(x, y) = p_i \cdot x + p_j \cdot y + p_k$$

$$\begin{bmatrix} p_i \\ p_j \\ p_k \end{bmatrix} = \begin{bmatrix} x_i & y_i & 1 \\ x_j & y_j & 1 \\ x_k & y_k & 1 \end{bmatrix}^{-1} \cdot \begin{bmatrix} w(x_i, y_i) \\ w(x_j, y_j) \\ w(x_k, y_k) \end{bmatrix} \quad (4)$$

The 3-D mosaicing gives correspondence at the control vertices between the input images and thus relative orientation can be executed if interior orientation parameters are known.

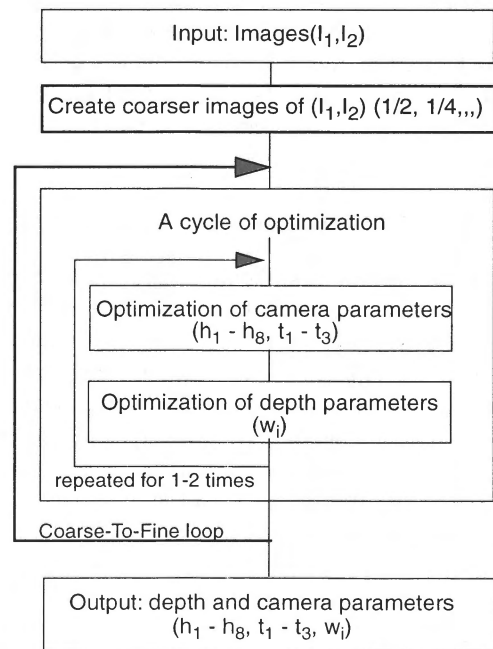


Figure 2: Flow chart of 3-D image registration

### 3. EXPERIMENT AND RESULT

#### 3.1 Implementation of 3-D Image Mosaicing

A prototype system of registration by 3-D image mosaicing has been developed. Figure 2 shows the flow chart of calculation of 3-D mosaicing parameters. First a series of images of  $I$  and  $I'$  are created for coarse-to-fine processing by reducing image size. Next,  $H(h_1, \dots, h_8)$  and  $(t_1, t_2, t_3)$  are estimated by LM method with the coarsest images and optimization of depth parameters follows. After repeating this optimization 1 or 2 times, processed images are exchanged to finer ones. These procedures are repeated until the finest (original) images are processed.

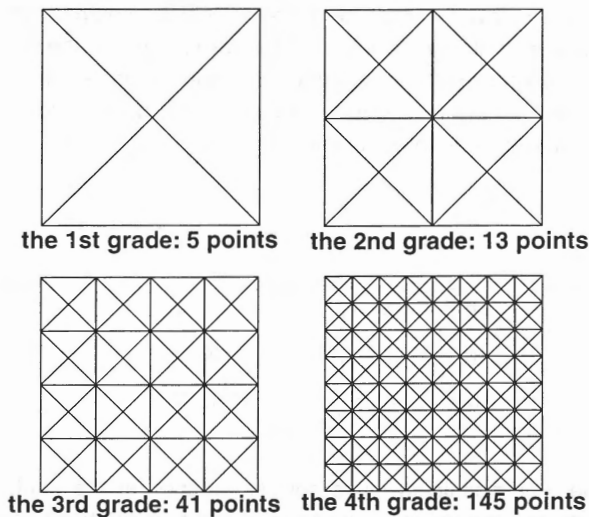


Figure 3: Control vertices and triangulation

Figure 3 illustrates the distribution of control vertices and triangles. Our program of 3-D mosaicing can specify a grade of control points at each stage of coarse-to-fine loop: the first grade control vertices contains only 5 points, while the 4th grade includes 145 control points. Higher grade of distribution should be specified for finer images in coarse-to-fine strategy.

#### 3.2 Results and Evaluation

**3.2.1 Depth Parameters:** Figure 4 and Figure 5 are the results of image registration by the 3-D mosaicing for two test cases 1 and 2. In each figure, the two images in the first row are original stereo pairs and the left image in the second row is the resultant depth parameters at each pixels. In the final results the control vertices were the 5th grade (545 points). Brighter pixels in these figures indicate larger (closer in these cases) depth parameters. Black parts indicate the part with no results. Most of them are the parts where image  $I$  had no matching points in  $I'$ , or where calculation error occurred.

Although the resultant depth maps show surface shape of the objects intuitively, considerable errors have occurred such as the parts indicated by the character A and B. The

parts indicated by A are because of calculation failure from lack of texture, while the parts indicated by B are because of unstable calculation since the direction of textures were along the epipolar line.

**3.2.2 Parameters  $H$  and  $(t_1, t_2, t_3)$ :** To check the precision of the camera parameters  $H(h_1, \dots, h_8)$  and  $(t_1, t_2, t_3)$  we have checked vertical parallax at check points showed in Figure 4 (4) and Figure 5 (4). As shown in Figure 6, vertical parallax for point  $P$  in  $I$  can be defined as the distance between the corresponding point  $P'$  and the epipolar line of  $P$ . The epipolar line lies on the epipole  $(t_1/t_3, t_2/t_3)$  and  $P_H$  on which  $P$  is projected by  $H$  in  $I'$ . After manual measurement of coordinates for all the check points in  $I$  and  $I'$ , vertical parallaxes for all points have been computed.

RMS errors of the vertical parallaxes are within 0.5 pixel for both of the test cases which concludes that the parameters  $H(h_1, \dots, h_8)$  and  $(t_1, t_2, t_3)$  have been computed rather precisely despite considerable errors are involved in depth parameters. This is important because the precision of relative orientation depends on the precision of parameter  $H(h_1, \dots, h_8)$  and  $(t_1, t_2, t_3)$ . This fact shows that image registration by the 3-D mosaicing is applicable to automatic relative orientation.

### 4. CONCLUSION

We have developed a prototype system which performs image registration by the 3-D mosaicing technique with stereo image pair and found that the method can be applied to automatic relative orientation. We are planning to improve our system so that more than two images can be processed at a time to utilize redundancy of stereo pairs.

### 5. REFERENCES

- Oda, K., Kano, H and Kanade, T., 1997. Generalized disparity and Its application for multi-stereo camera calibration, Optical 3-D, pp.109-116.
- Press, W.H., et al., 1992. Numerical Recipes in C: The Art of Scientific Computing, Cambridge University Press, Cambridge, England, Second Editing.
- Szeliski, R., 1994. Image Mosaicing for Tele-Reality Applications, DEC CRL 94/1.
- Szeliski, R., and Kang, S.B, 1995. Direct Methods for Visual Scene Reconstruction, the Workshop on Representation of Visual Scenes (VSR 95).

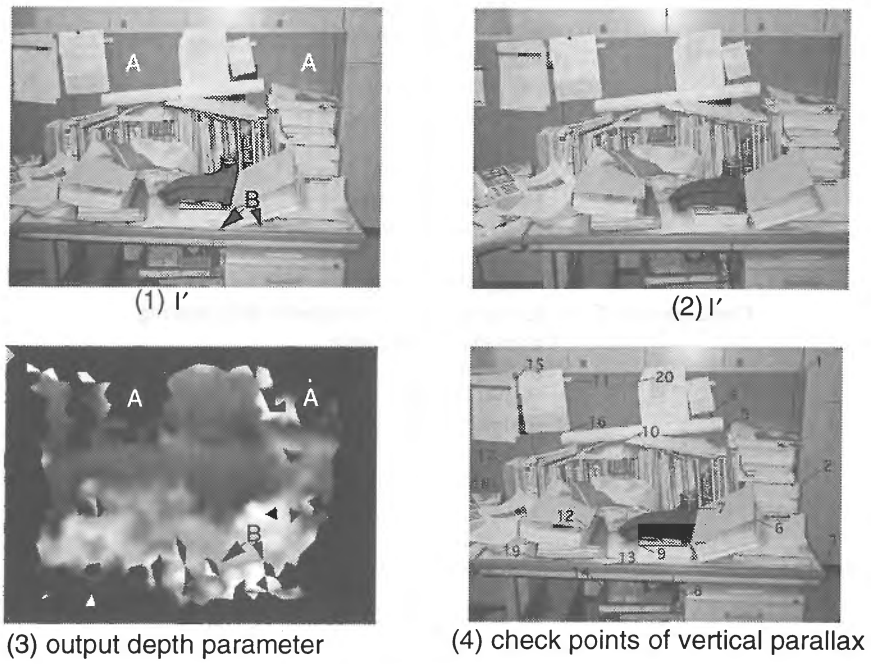


Figure 4: Result of image registration by 3-D mosaicing - Test case 1

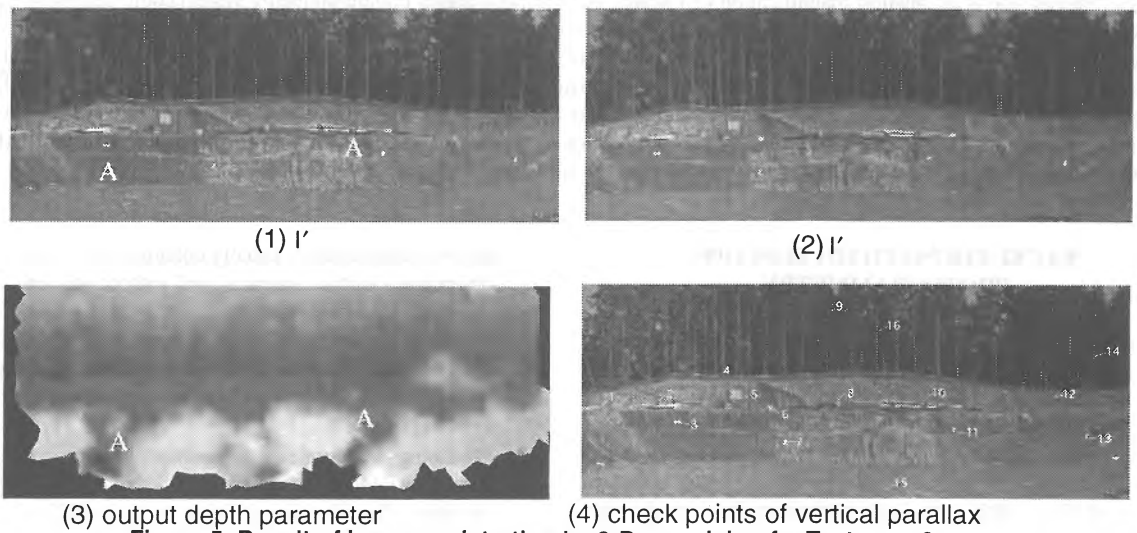


Figure 5: Result of image registration by 3-D mosaicing for Test case 2

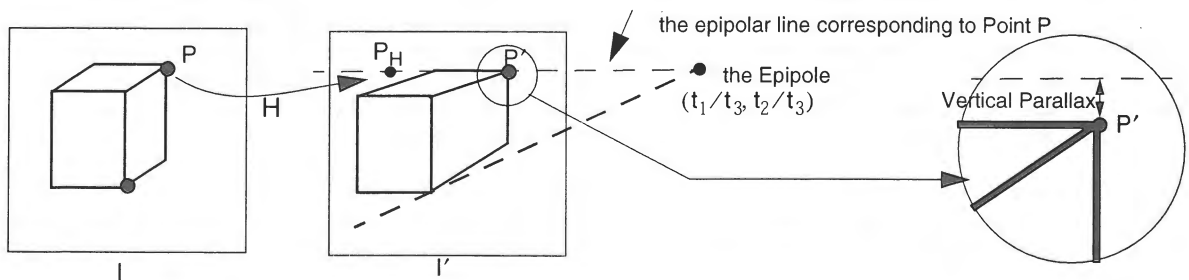


Figure 6: Vertical parallax and epipole